Hindawi
Complexity
Volume 2019, Article ID 6317270, 10 pages
https://doi.org/10.1155/2019/6317270

Research Article

Fuel Cell Output Current Prediction with a Hybrid Intelligent System

José-Luis Casteleiro-Roca,[1] **Antonio Javier Barragán**,[2] **Francisca Segura**,[2] **José Luis Calvo-Rolle**,[1] **and José Manuel Andújar**[2]

[1] *University of A Coruña, Department of Industrial Engineering, Avda. 19 de febrero s/n, 15495 Ferrol, A Coruña, Spain*
[2] *University of Huelva, Department of Electronic Engineering, Computer Systems and Automatic, Campus de El Carmen, 21071 Huelva, Spain*

Correspondence should be addressed to José-Luis Casteleiro-Roca; jose.luis.casteleiro@udc.es

Received 26 October 2018; Revised 23 December 2018; Accepted 29 January 2019; Published 12 February 2019

Guest Editor: Izaskun Garrido

A fuel cell is a complex system, which produces electricity through an electrochemical reaction. For the formal application of control strategies on a fuel cell, it is very important to have a precise dynamic model of it. In this paper, a dynamic model of a real hydrogen fuel cell is obtained to predict its response. The data used in this paper to obtain the model have been acquired from a real fuel cell subjected to different load patterns by means of a programmable electronic load. Using this data, a nonlinear model based on a hybrid intelligent system is obtained. This hybrid model uses artificial neural networks to predict the output current of the fuel cell in a very precise way. The use of a hybrid scheme improves the performance of neural networks reducing to half the mean squared error obtained for a global model of the fuel cell.

1. Introduction

The problems derived from pollution, and the increasingly alarming climate change, have led modern society to look for clean energy sources. One of the most promising technologies for accomplishing hybrid energy topologies is based on renewable sources centers on hydrogen, due to its possible generation by electrolysers and then its storage. Subsequently, from this gas, the generation of electrical energy by fuel cells is absolutely feasible [1]. In this sense, fuel cell based systems are an energy source that appears as a hopeful choice as a result of their increased performance, high reliability in steady applications, and small environmental incidence, space and automotive applications [2].

A fuel cell is a complex system consisting of a series connection of individual cells (a stack), where the electric current is produced by an electrochemical reaction, combined with all other systems necessary for its operation, that is, filters and systems that condition the gases involved in the reaction (H_2 and O_2), a cooling system, and, of course, a control system [3]. Compared to other clean technologies, such as wind or photovoltaic generation, fuel cells do not require a specific location to obtain higher performance. In addition, they are very respectful of the environment. Proton Exchange Membrane (PEM) fuel cells (PEMFC) offer high energy density and a number of advantages, such as their low volume and weight compared to other technologies. PEMFC operate at low temperatures (50°C–100°C), which allow them to start more quickly (requiring less heating time), and result in less wear and tear on system components and better durability. PEMFC are commercially available in a large range of powers (from some watts to several MW), permitting their use in a large number of applications [2]. For example, in stationary applications, fuel cells can be connected to the electrical network [4], installed as separate generators [5], or operate in landfills and wastewater treatment plants [6]. Its use is also interesting in transport applications, owing to the scarcity of fossil fuels and their polluting effects [7, 8], or on other types of mobile stations [9].

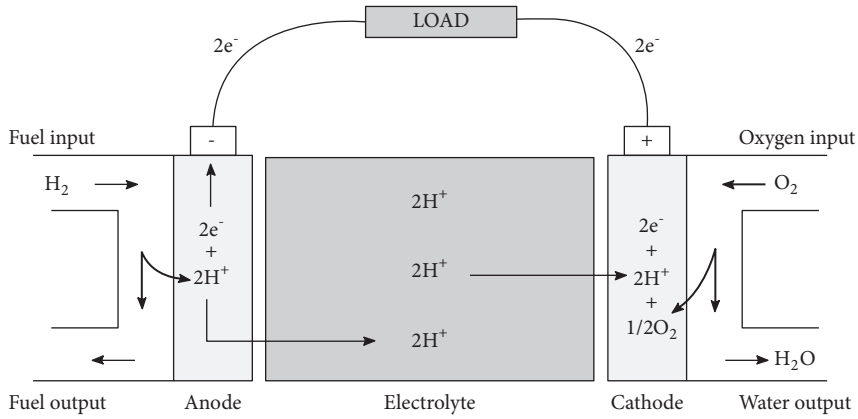

Figure 1: Fuel cell diagram.

A fuel cell behaves as a nonlinear dynamical system, which generates electrical energy through an electrochemical reaction. The energy generated by the fuel cell is not regulated; thus, a control system is necessary for its efficient use [10–13]. In this way, for the formal application of control strategies on a fuel cell, it is very important to have a model of its dynamic behaviour [1, 14–18]. Hou et al. [19] analysed stack voltage response to current steps measuring voltage variation rate, initial value of dynamic voltage, time to reach steady state and dynamic resistance factor. The results of this investigation show that the dynamic response of the stack voltage is different for increases and decreases in current [20], what must be taken into account when establishing a test pattern to obtain data from the fuel cell.

It is important to be able to predict the behaviour of fuel cells for their efficient use; hence, obtaining an accurate model is a very important task before designing a control strategy. Achieving an accurate model of a system is a fundamental part of its study; however, we do not always have enough information to obtain an acceptable mathematical model. Therefore, we must resort to modelling techniques based on input–output data [21–25]. In control systems this process is even more critical, since it requires a model as accurate as possible, both to perform analysis on the system [26–28] and to design a suitable and efficient controller for it [29–31].

For the current prediction in this paper, several regression techniques had been checked. The algorithms based on multiple regression analysis are accepted regression methods used in several applications [32–37]. Some previous works have shown the use of these methods despite its low performance [33, 38–40]. In this paper, to overcome this limitation, we propose to use hybrid intelligent system to accomplish the regression task, more specifically, an artificial neural network (ANN) hybrid system as the ones used in [41–46], since ANNs allow obtaining simple and very accurate nonlinear models [47–50].

This work is divided into the following sections. After to the current introduction, the case study is described in detail. Afterwards, the model approach and the employed algorithms are presented. The results section explains the best achieved configuration of the hybrid model, and the validation of the accomplished prediction model. Lastly, conclusions are explained and future works are depicted.

2. Case of Study

A single fuel cell of a PEM stack consists of an electrolyte layer in contact with an anode and a cathode on both sides; see Figure 1 . A PEM fuel cell produces electrochemical energy when a hydrogen-rich gas passes through the anode and a gas rich in oxygen (or air) passes through the cathode with an electrolyte between the anode and the cathode, which allows the exchange of electrical charge (ions) [51]. The dissociation of hydrogen molecules produces the flow of ions through the electrolyte and an electric current through an external circuit. The only residue generated is pure water. A usual single fuel cell produces approximately 1.2 V under normal operating conditions. For the creation of higher power systems, cells are connected in series forming a stack.

The data used for the realisation of the model were acquired through laboratory tests of an air-cooled polymer electrolyte fuel cell (AC-PEFC). Specifically, a PEM FCgen-1020AVS stack from Ballard was used [52]. This stack was built with 80 BAM4G cells [53] based on polymeric composition. The anode and cathode side are made of a porous carbon cloth with a catalyst based on platinum and platinum-ruthenium [54]. The stack was assembled with graphite plates and sandwiched between aluminium end plates by compression. The PEM FCgen-1020AVS stack is designed to provide up to 3.4 kW stable nonregulated electrical power with 45.33 V and 75 A. This stack is air-cooled, and a dead-ended configuration is used; thus, it does not require external humidification of the air or hydrogen. The inlet hydrogen pressure can vary from 1.16 to 1.56 bar. The oxidant and cooling subsystem were built based on the manufacturer's instructions [55]. The complete sequence to put into operation the individual devices that make up the stack, the oxidation and cooling subsystem, the electric subsystem, and the implementation of the balance of plant (BoP), whose schema is shown in Figure 2 and a real image of the laboratory in Figure 3, were thoroughly explained in [56].

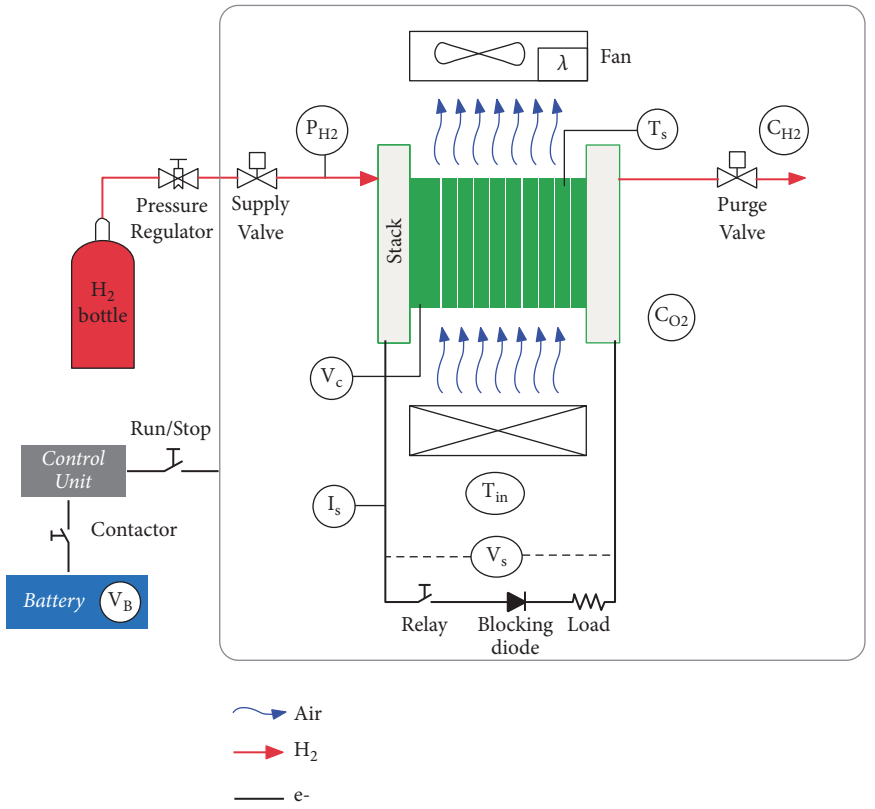

Figure 2: Stack + BoP to integrate the fuel cell.

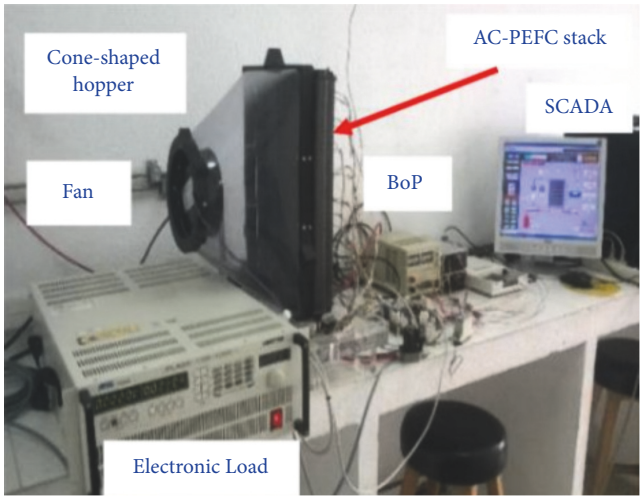

Figure 3: Laboratory implementations to test the fuel cell.

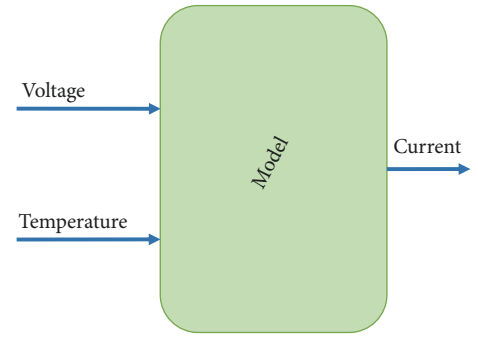

Figure 4: Basic schematic model.

To test the system an Amrel PLA5K-120-1200 programmable electronic load was used. A system was implemented to monitor all the fuel cell systems and store the data resulting from the tests, which was described in [57, 58]. In [59], a detailed thermal model based on differential equations is established according to the conservation equations of mass and energy for a 16 cells PEMFC stack. In this work, the effects of the temperature on the operation of the cell are demonstrated. In order to avoid these effects of operation, the used BoP includes a temperature control system to guarantee the maintenance of the fuel cell at its optimum value. In addition, it is necessary to keep in mind that the hydrogen gas should be vented periodically to the atmosphere and replaced with fresh hydrogen using a purge process according to [55].

3. Model Approach

The model proposal implemented in this work is illustrated in Figure 4, where the inputs are the voltage and the temperature measured at the BoP and the output is the present value of the current. To take into account the process dynamic, the inputs

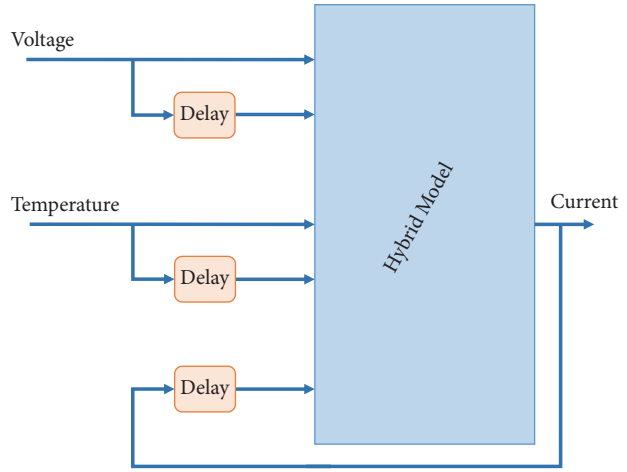

Figure 5: Model approach to predict actual current value.

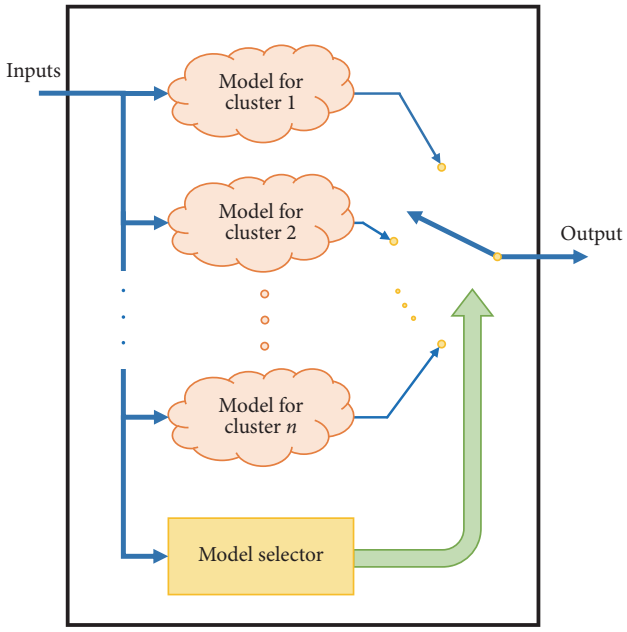

Figure 6: Internally schematic to achieve the hybrid model.

of the model include the previous measured values of voltage, temperature, and current.

An internal layout of the model with the mentioned previous variable values is shown in Figure 5, where the hybrid model is represented. Due to the possible nonlinear response, this hybrid model is built upon clustering; the modelling dataset is divided in groups with similar characteristics. A different regression model was created for each cluster with the objective to increase the whole model performance.

Figure 6 represents the operation of the hybrid model shown in Figure 5. The number of clusters is obtained by testing different topologies. This figure represents a general hybrid model, with n clusters and n models with the specific parameters for each one.

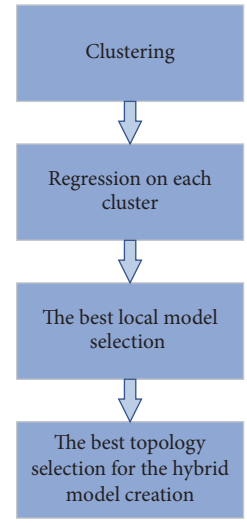

Figure 7: Flowchart of the hybrid model creation phases.

To create a hybrid model, the modelling process could be divided into the following steps (Figure 7):

(1) Clustering phase

(2) Regression modelling phase for each cluster

(3) Selection of the best local model (by cluster)

(4) Selection of the best topology for the hybrid model

For the clustering phase, the k-means algorithm has been used to achieve the groups with similar features. To perform the regression modelling phase, the ANN algorithm was chosen considering its capacity to predict the output of nonlinear systems with a simple internal configuration. Although this is a hybrid system, the model achieves better results if the regression algorithms are intelligent systems than if they are traditional regression methods. The regression modelling phase uses k-fold to achieve a more real approach in the model performance measurement. The k-fold testing method is explained in Figure 8. The data for each cluster is divided into k times and k models with the same configuration and are trained with different test data.

As it is shown in Figure 8, the errors values between the measured and the predicted output for each model are stored. When the k-fold process finished, all the data of a specific cluster is used to test the model, and the performance could be achieved. When all the different possible configurations for the models are tested, the best regression algorithm for each group is chosen based on the lowest error reached.

For the hybrid model topology definition, the number of clusters must be determined. This choice is done based on the global error considering the samples quantity for every cluster and estimating a weighted error. The best hybrid configuration is the one with the best whole performance.

3.1. K-Means Algorithm. The k-means method is used to create a certain number of groups in an unlabeled data set. The idea is to place centroids in the corresponding hyperspace, so that the data belonging to the same centroid

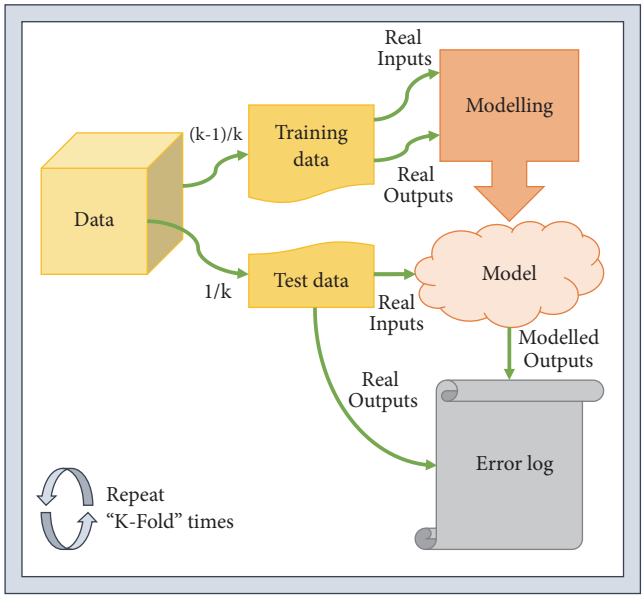

Figure 8: K-Fold training and test data selection.

have similar characteristics and represent a data cluster [60, 61].

Every new sample, once the centroids are trained and correctly placed in the hyperspace, is compared with them and is associated with the centroid that is closest in terms of the chosen distance, usually the Euclidean [62].

This algorithm has an initial training phase that needs to know the number of clusters to divide the data. This phase could be slow depending on the number of groups and the data size; however, once the training is finished, the cluster assignment is very fast for new data [63].

The initial location of the centroids is chosen randomly. Then, the location varies, until reaching the greatest distance between them, according to the following procedure:

(i) Each sample is associated with the nearest centroid and is included in a specific list.

(ii) After checking all the samples and being associated with the list of the corresponding centroid, the list of labelled samples will be available.

(iii) The location of the centroid is recalculated obtaining the center of the set of samples that have been associated with it.

(iv) The procedure is repeated until the centroids are no longer displaced in the successive calculations.

Moreover, as the initial centroids are randomly selected, the procedure is repeated several times until the largest distance between centroids is reached.

3.2. Artificial Neural Networks. The ANN is an intelligent algorithm that uses small processing units called neurons. These neurons are interconnected between each other through links, and each one calculates a function taking into account the different inputs. All the inputs to each neuron have its weight in the activation function inside the neuron [64].

The main specific characteristics of ANNs are that they can learn from experience through the generalization of cases [65]. The ANNs are adaptive intelligent systems that can carry out certain functions through training. The ANNs create their own internal representation of the problem with the training and respond according to the situations, although they had not previously learned a specific situation. Then, the ANNs are able to generalize from previous cases to new ones [66].

The activation function defines the new state, or output, of the neuron as level of excitation [67]. The activation degree of the artificial neuron can usually vary between a range (normally [0, 1] or [-1, 1]). This value indicates the state of the neuron: inactive (0 or -1), active (1), or an intermediate state between these limits which indicates its activation degree.

The topology, or architecture, of an ANN is determined by the organization of the neurons, their arrangement, and their connections. The architecture depends on four main parameters: the layers quantity in the system, the number of neurons of every layer, the connectivity between neurons, and the activation functions [68].

The basic structure to interconnect neurons is the multilayer perceptron. This type of ANN is organized in several layers: input, intermediate or hidden and output. A layer is a set of neurons whose input information comes from the same source: the inputs of the ANN for the input layer or the previous layer for the rest of the layers. The output of the neurons in the same layer has the same destination too: the next layer or the output of the ANN (in the case of the output layer).

Normally, the output layer neurons use special activation functions depending on the use of the ANN; for regression, the typical is the linear function.

3.3. Data Processing. The data set in this research is collected using the BoP system described in the case study section. With this equipment, the samples from two different days were collected. A total of 774391 samples were recorded from these tests and, after discarding the bad measurements, the data sets were reduced to 774,385. As the model used previous values, it was necessary to eliminate the samples that did not have all the inputs values to model.

Although there were 774,379 valid samples, only 1/5 of them were used to train the hybrid model; they were selected randomly to ensure the generalization of the model. Then, only 154,875 samples were used in the modelling phase.

In addition, the samples of another different day were used to validate the hybrid model achieved. 4,832 samples, which were not used in the modelling phase, were recorded from two separate tests (1,489 and 3,343 samples each), and they were used in the validation phase of the research.

4. Results

The results of this research could be divided into three different parts: the clustering, the modelling, and the validation.

4.1. Clustering Results. The clusters were created with the explained k-means algorithm. Nine hybrid systems were created with different number of clusters (between 2 and 9),

Table 1: Number of samples in each created cluster.

	Cl-1	Cl-2	Cl-3	Cl-4	Cl-5	Cl-6	Cl-7	Cl-8	Cl-9	Cl-10
Global	154,875									
Hybrid 2	*75,814*	*79,061*								
Hybrid 3	47,719	50,414	56,742							
Hybrid 4	10,699	37,213	50,414	56,549						
Hybrid 5	10,699	28,324	30,251	37,020	48,581					
Hybrid 6	10,699	22,194	28,058	28,324	28,580	37,020				
Hybrid 7	285	10,699	22,194	28,084	28,273	28,320	37,020			
Hybrid 8	285	2,627	10,475	22,194	28,084	28,273	28,320	34,617		
Hybrid 9	285	2,627	5,375	8,161	22,194	27,538	28,084	28,250	32,361	
Hybrid 10	285	2,027	2,627	5,099	8,161	22,194	26,447	27,533	28,139	32,363

Table 2: Configuration for each individual hybrid model.

	Cl-1	Cl-2	Cl-3	Cl-4	Cl-5	Cl-6	Cl-7	Cl-8	Cl-9	Cl-10
Global	ANN15									
Hybrid 2	*ANN15*	*ANN12*								
Hybrid 3	ANN14	ANN11	ANN12							
Hybrid 4	ANN14	ANN15	ANN14	ANN11						
Hybrid 5	ANN11	ANN13	ANN11	ANN14	ANN15					
Hybrid 6	ANN12	ANN13	ANN15	ANN12	ANN15	ANN12				
Hybrid 7	ANN11	ANN14	ANN12	ANN12	ANN11	ANN12	ANN13			
Hybrid 8	ANN11	ANN15	ANN11	ANN11	ANN11	ANN11	ANN12	ANN14		
Hybrid 9	ANN11	ANN15	ANN13	ANN11	ANN12	ANN13	ANN11	ANN12	ANN15	
Hybrid 10	ANN11	ANN13	ANN11	ANN13	ANN11	ANN12	ANN12	ANN15	ANN11	ANN15

Table 3: Mean square error for each individual hybrid model.

	Cl-1	Cl-2	Cl-3	Cl-4	Cl-5	Cl-6	Cl-7	Cl-8	Cl-9	Cl-10
Global	0.0043									
Hybrid 2	*0.0014*	*0.0028*								
Hybrid 3	0.0012	0.0046	0.0030							
Hybrid 4	0.0000	0.0010	0.0069	0.0046						
Hybrid 5	0.0000	0.0000	0.0102	0.0032	0.0144					
Hybrid 6	0.0000	0.0146	0.0037	0.0000	0.0085	0.0010				
Hybrid 7	0.0000	0.0000	0.0147	0.0034	0.0058	0.0000	0.0014			
Hybrid 8	0.0000	0.0075	0.0000	0.0184	0.0031	0.0017	0.0000	0,0003		
Hybrid 9	0.0000	0.0075	0.0000	0.0000	0.0171	0.0000	0.0030	0.0082	0.0002	
Hybrid 10	0.0000	0.0000	0.0075	0.0000	0.0000	0.0041	0.0000	0.0074	0.0019	0.0000

as the optimal number of groups was previously unknown. The algorithm was trained with random initialisation of the centroids, and the training was repeated 20 times to ensure the best divisions, the furthest centroids. The number of samples used in the modelling phase for each cluster is shown in Table 1.

4.2. Modelling Results. The ANN regression algorithm is configured with only a single hidden layer. The input layer has 5 inputs, one for each variable explained in the model approach section, and only 1 output in the last layer. Several configurations of the ANNs for each cluster were trained, all of them with tan-sigmoid activation function for the internal neurons (in the hidden layer) and, in the output layer, a linear activation function was used. The difference in the several configurations was the hidden layer neurons' quantity. This layer size varied from 1 to 15 neurons.

To train each ANN configuration, the Levenberg-Marquardt optimization algorithm was used. Moreover, to finish the training phase, gradient descent was used base on the MSE (mean squared error). The best ANN configurations for each cluster are indicated in Table 2.

The selection of these advantageous configurations uses the MSE as a performance measurement for the created models. In Table 3 it is possible to see the lowest error for

Table 4: Mean squared error for each model.

	Global	Hybrid model (local models)								
		2	3	4	5	6	7	8	9	10
MSE	0.0043	*0.0021*	0.0030	0.0042	0.0073	0.0046	0.0041	0.0037	0.0047	0.0024

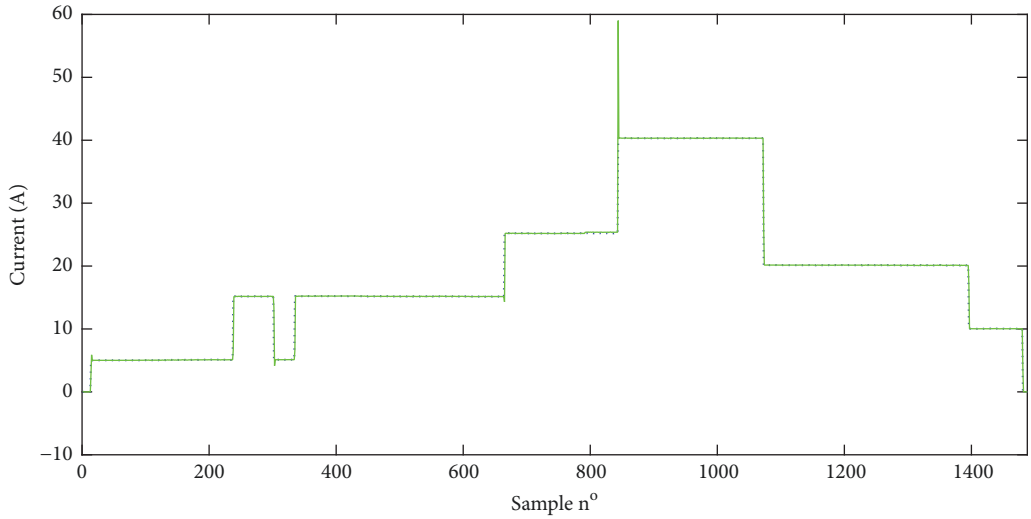

Figure 9: Validation test 1.

Table 5: Performance values for the validation tests.

	MSE	NMSE	MAE	MAPE
Validation test 1	0.5327	0.0043	0.0704	1.9414
Validation test 2	0.4384	8.4272e-4	0.1889	3.7677

each cluster achieved with the configuration that is shown in Table 2.

To calculate the best hybrid configuration for the whole model, as explained, the number of samples was considered. The performance of the different hybrids and the global model is presented in Table 4. It is shown that the best configuration implies a hybrid model with two clusters, and the error using a global model is more than the double.

4.3. Validation Procedure. Two validation data sets were used to check the final hybrid model accomplished with 2 clusters and configurations of 15 and 12 internal neurons. The first test is shown in Figure 9, where the current has few changes, but it is possible to appreciate that the real data (blue dotted line) and the output of the model (green continuous line) are very close all the time.

The second validation data set (Figure 10) shows a usual test for the fuel cells. In this case, the current is increased until its maximum and, then, reduced gradually. The predicted value in this case shows the biggest error in the middle of the test when the current has the highest values.

In Table 5 different error values are shown for the validation data: MSE, NMSE (normalize mean square error), MAE (mean absolute error), and MAPE (mean absolute percentage error). Despite the graphical error shown for the second validation data in Figure 10, the error values are very good. The worst value is the MAE because, in the test, the current has very high values; however, the other error values are lower than the ones obtained in the first validation data. This fact could be confirmed with Figure 11, where the percentage absolute error of the second validation data is in the worst part of the test (the central part of Figure 10).

5. Conclusions

A model of a fuel cell based on hydrogen has been developed in this work. The model predicts the current in the fuel cell under different working points, and it could be used in several ways as control or fault detection. As an example, in the fault detection field, the model output must be similar to the real measure of a current sensor, and if the measured value deviates from the modelled one, a sensor failure or a system malfunction could be represented.

Since the fuel cell is a nonlinear system, a hybrid model instead of a global is selected. In this paper, ANNs are used as regression algorithm due to its accuracy. Furthermore, with the hybrid model, the performance of the ANNs is increased up reducing to half the MSE obtained with a global model.

Very good results are obtained in terms of error in the predicted current considering that the MSE value is 0.0021 for the hybrid model with 2 clusters. One of them used an ANN with 15 internal neurons and the other an ANN with 12 neurons. To validate the model, two different data sets were used and, although the maximum MAE was 0.1889, the maximum NMSE was only 0.0043.

As for future works, the possibility of predicting the future values of the current will be examined. This future prediction

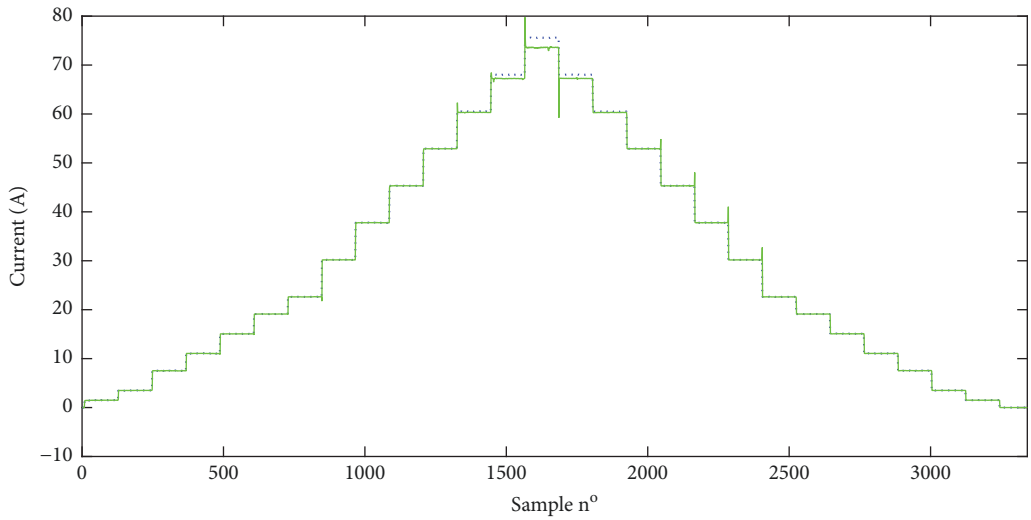

Figure 10: Validation test 2.

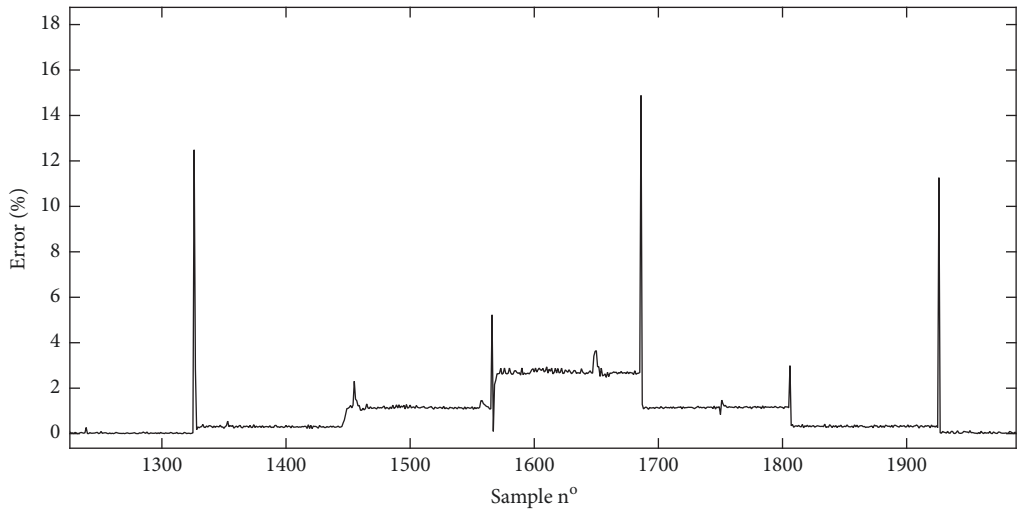

Figure 11: Percentage absolute error in the worst part of the validation test 2.

would increase the fuel cell performance, since it could be adapted faster to new working points.

Data Availability

The data used to support the findings of this study are available from the corresponding author upon request.

Conflicts of Interest

The authors declare that they have no conflicts of interest.

Acknowledgments

This work has been funded by the Spanish Ministry of Economy Industry and Competitiveness through the H2SMART-μGRID (DPI2017-85540-R) project.

References

[1] F. Vivas, A. De las Heras, F. Segura, and J. Andújar, "A review of energy management strategies for renewable hybrid energy systems with hydrogen backup," *Renewable & Sustainable Energy Reviews*, vol. 82, pp. 126–155, 2018.

[2] J. Andújar and F. Segura, "Fuel cells: History and updating. A walk along two centuries," *Renewable & Sustainable Energy Reviews*, vol. 13, no. 9, pp. 2309–2322, 2009.

[3] A. De las Heras, F. Vivas, F. Segura, and J. Andújar, "From the cell to the stack. A chronological walk through the techniques to manufacture the PEFCs core," *Renewable & Sustainable Energy Reviews*, vol. 96, pp. 29–45, 2018.

[4] M. V. Moreira and G. E. da Silva, "A practical model for evaluating the performance of proton exchange membrane fuel cells," *Journal of Renewable Energy*, vol. 34, no. 7, pp. 1734–1741, 2009.

[5] A. Kirubakaran, S. Jain, and R. K. Nema, "A review on fuel cell technologies and power electronic interface," *Renewable and Sustainable Energy Reviews*, vol. 13, no. 9, pp. 2430–2440, 2009.

[6] J. Paska, P. Biczel, and M. Kłos, "Hybrid power systems – An effective way of utilising primary energy sources," *Journal of Renewable Energy*, vol. 34, no. 11, pp. 2414–2421, 2009.

[7] M. Bertoluzzo and G. Buja, "Development of electric propulsion systems for light electric vehicles," *IEEE Transactions on Industrial Informatics*, vol. 7, no. 3, pp. 428–435, 2011.

[8] A. De las Heras, F. Vivas, F. Segura et al., "Air-cooled fuel cells: Keys to design and build the oxidant/cooling system," *Journal of Renewable Energy*, vol. 125, pp. 1–20, 2018.

[9] D. Ross, "Power struggle [power supplies for portable equipment]," *IEE Review*, vol. 49, no. 7, pp. 34–38, 2003.

[10] J. Andújar, F. Segura, E. Durán, and L. Rentería, "Optimal interface based on power electronics in distributed generation systems for fuel cells," *Journal of Renewable Energy*, vol. 36, no. 11, pp. 2759–2770, 2011.

[11] F. Segura, J. M. Andújar, and E. Durán, "Analog current control techniques for power control in PEM fuel-cell hybrid systems: A critical review and a practical application," *IEEE Transactions on Industrial Electronics*, vol. 58, no. 4, pp. 1171–1184, 2011.

[12] J. Lekube, A. J. Garrido, I. Garrido, and E. Otaola, "Output power improvement in oscillating water column-based wave power plants," *Revista Iberoamericana de Automatica e Informatica Industrial (RIAI)*, vol. 15, no. 2, pp. 145–155, 2018.

[13] J.-L. Casteleiro-Roca, E. Jove, F. Sánchez-Lasheras et al., "Power cell SOC modelling for intelligent virtual sensor implementation," *Journal of Sensors*, vol. 2017, Article ID 9640546, 10 pages, 2017.

[14] J. C. Amphlett, R. M. Baumert, R. F. Mann et al., "Performance modeling of the ballard Mark IV solid polymer electrolyte fuel cell I. mechanistic model development," *Journal of The Electrochemical Society*, vol. 142, no. 1, pp. 1–8, 1995.

[15] J. C. Amphlett, R. F. Mann, B. A. Peppley et al., "A model predicting transient responses of proton exchange membrane fuel cells," *Journal of Power Sources*, vol. 61, no. 1-2, pp. 183–188, 1996.

[16] P. Famouri and R. Gemmen, "Electrochemical circuit model of a PEM fuel cell," in *Proceedings of the IEEE Power Engineering Society General Meeting*, vol. 3, pp. 1436–1440, IEEE, Toronto, Canada, 2003.

[17] J. Kim, S.-M. Lee, S. Srinivasan, and C. E. Chamberlin, "Modeling of proton exchange membrane fuel cell performance with an empirical equation," *Journal of The Electrochemical Society*, vol. 142, no. 8, pp. 2670–2674, 1995.

[18] H. P. van Bussel, F. G. Koene, and R. K. Mallant, "Dynamic model of solid polymer fuel cell water management," *Journal of Power Sources*, vol. 71, no. 1-2, pp. 218–222, 1998.

[19] Y. Hou, Z. Yang, and X. Fang, "An experimental study on the dynamic process of PEM fuel cell stack voltage," *Journal of Renewable Energy*, vol. 36, no. 1, pp. 325–329, 2011.

[20] C. Ziogou, S. Voutetakis, S. Papadopoulou, and M. C. Georgiadis, "Modeling, simulation and experimental validation of a PEM fuel cell system," *Computers & Chemical Engineering*, vol. 35, no. 9, pp. 1886–1900, 2011.

[21] A. J. Barragán, B. M. Al-Hadithi, A. Jiménez, and J. M. Andújar, "A general methodology for online TS fuzzy modeling by the extended Kalman filter," *Applied Soft Computing*, vol. 18, pp. 277–289, 2014.

[22] M. J. López-Baldán, A. García-Cerezo, J. M. López, and A. R. Gallego, "Fuzzy modeling of a thermal solar plant," *International Journal of Intelligent Systems*, vol. 17, no. 4, pp. 369–379, 2002.

[23] S. O. T. Ogaji, R. Singh, P. Pilidis, and M. Diacakis, "Modelling fuel cell performance using artificial intelligence," *Journal of Power Sources*, vol. 154, no. 1, pp. 192–197, 2006.

[24] S. Wojciechowski, "A comparison of classification strategies in rule-based classifiers," *Logic Journal of the IGPL*, vol. 26, no. 1, pp. 29–46, 2018.

[25] F. Segovia, J. M. Górriz, J. Ramírez et al., "Using deep neural networks along with dimensionality reduction techniques to assist the diagnosis of neurodegenerative disorders," *Logic Journal of the IGPL*, vol. 26, no. 6, pp. 618–628, 2018.

[26] A. J. Barragán, B. M. Al-Hadithi, J. M. Andújar, and A. Jiménez, "Formal methodology for analyzing the dynamic behavior of nonlinear systems using fuzzy logic," *Revista Iberoamericana de Automatica e Informatica Industrial (RIAI)*, vol. 12, no. 4, pp. 434–445, 2015.

[27] F. Gordillo, J. Aracil, and T. Alamo, "Determining limit cycles in fuzzy control systems," in *Proceedings of the 6th International Fuzzy Systems Conference*, vol. 1, pp. 193–198, IEEE, Barcelona, Spain, 1997.

[28] X. M. Vilar-Martínez, J. A. Montero-Sousa, J. L. Calvo-Rolle, and J. L. Casteleiro-Roca, "Expert system development to assist on the verification of "tacan" system performance," *Dyna*, vol. 89, no. 1, pp. 112–121, 2014.

[29] J. G. Fontanet, A. L. Cervantes, and I. B. Ortiz, "Alternatives of control for a furuta's pendulum," *Revista Iberoamericana de Automática e Informática Industrial RIAI*, vol. 13, no. 4, pp. 410–420, 2016.

[30] E. Irigoyen and G. Miñano, "A NARX neural network model for enhancing cardiovascular rehabilitation therapies," *Neurocomputing*, vol. 109, pp. 9–15, 2013.

[31] J. Marquez, A. Pina, and M. Arias, "A general and formal methodology to design stable nonlinear fuzzy control systems," *IEEE Transactions on Fuzzy Systems*, vol. 17, no. 5, pp. 1081–1091, 2009.

[32] A. Ghanghermeh, G. Roshan, J. Orosa et al., "New climatic indicators for improving urban sprawl: A case study of tehran city," *Entropy*, vol. 15, no. 3, pp. 999–1013, 2013.

[33] J. L. Calvo-Rolle, H. Quintian-Pardo, E. Corchado, M. del Carmen Meizoso-López, and R. Ferreiro García, "Simplified method based on an intelligent model to obtain the extinction angle of the current for a single-phase half wave controlled rectifier with resistive and inductive load," *Journal of Applied Logic*, vol. 13, no. 1, pp. 37–47, 2015.

[34] J. L. Calvo-Rolle, O. Fontenla-Romero, B. Pérez-Sánchez, and B. Guijarro-Berdinas, "Adaptive inverse control using an online learning algorithm for neural networks," *Informatica*, vol. 25, no. 3, pp. 401–414, 2014.

[35] E. Jove, J. M. Gonzalez-Cava, J. Casteleiro-Roca et al., "Modelling the hypnotic patient response in general anaesthesia using intelligent models," *Logic Journal of the IGPL*, 2018.

[36] E. Jove, J. A. Lopez-Vazquez, M. I. Fernandez-Ibanez et al., "Hybrid intelligent system to predict the individual academic performance of engineering students," *International Journal of Engineering Education*, vol. 34, no. 3, pp. 895–904, 2018.

[37] E. Jove, P. Blanco-Rodrguez, J. L. Casteleiro-Roca et al., "Attempts prediction by missing data imputation in engineering degree," in *Proceeding of the International Joint Conference SOCO'17-CISIS'17-ICEUTE'17*, pp. 167–176, Springer, León, Spain, 2017.

[38] J. L. Casteleiro-Roca, J. L. Calvo-Rolle, M. C. Meizoso-López, A. J. Piñón-Pazos, and B. A. Rodríguez-Gómez, "Bio-inspired model of ground temperature behavior on the horizontal geothermal exchanger of an installation based on a heat pump," *Neurocomputing*, vol. 150, pp. 90–98, 2015.

[39] I. Machón-González, H. López-García, and J. L. Calvo-Rolle, "A hybrid batch SOM-NG algorithm," in *Proceedings of the International Joint Conference on Neural Networks (IJCNN)*, pp. 1–5, IEEE, Barcelona, Spain, 2010.

[40] J. A. Rincon, V. Julian, C. Carrascosa et al., "Detecting emotions through non-invasive wearables," *Logic Journal of the IGPL*, vol. 26, no. 6, pp. 605–617, 2018.

[41] R. F. Garcia, J. L. Rolle, M. R. Gomez, and A. D. Catoira, "Expert condition monitoring on hydrostatic self-levitating bearings," *Expert Systems with Applications*, vol. 40, no. 8, pp. 2975–2984, 2013.

[42] J. L. Calvo-Rolle, J. L. Casteleiro-Roca, H. Quintián, and M. Del Carmen Meizoso-Lopez, "A hybrid intelligent system for PID controller using in a steel rolling process," *Expert Systems with Applications*, vol. 40, no. 13, pp. 5188–5196, 2013.

[43] R. Ferreiro Garcia, J. L. Rolle, J. P. Castelo, and M. R. Gomez, "On the monitoring task of solar thermal fluid transfer systems using NN based models and rule based techniques," *Engineering Applications of Artificial Intelligence*, vol. 27, pp. 129–136, 2014.

[44] H. Quintián, J. L. Calvo-Rolle, and E. Corchado, "A hybrid regression system based on local models for solar energy prediction," *Informatica*, vol. 25, no. 2, pp. 265–282, 2014.

[45] H. Q. Pardo, J. L. C. Rolle, and O. F. Romero, "Application of a low cost commercial robot in tasks of tracking of objects," *Dyna*, vol. 79, no. 175, pp. 24–33, 2012.

[46] A. Moreno-Fernandez-de Leceta, J. M. Lopez-Guede, L. Ezquerro Insagurbe et al., "A novel methodology for clinical semantic annotations assessment," *Logic Journal of the IGPL*, vol. 26, no. 6, pp. 569–580, 2018.

[47] H. Alaiz Moretón, J. L. Calvo Rolle, I. García, and A. Alonso Alvarez, "Formalization and practical implementation of a conceptual model for PID controller tuning," *Asian Journal of Control*, vol. 13, no. 6, pp. 773–784, 2011.

[48] J. Rolle, I. Gonzalez, and H. Garcia, "Neuro-robust controller for non-linear systems," *Dyna*, vol. 86, no. 3, pp. 308–317, 2011.

[49] J. L. Casteleiro-Roca, J. A. M. Pérez, A. J. Piñón-Pazos et al., "Modeling the electromyogram (emg) of patients undergoing anesthesia during surgery," in *Proceeding of the International Conference on Soft Computing Models in Industrial and Environmental Applications*, pp. 273–283, Springer, 2015.

[50] R. F. Garcia, J. L. C. Rolle, J. P. Castelo, and M. R. Gomez, "On the monitoring task of solar thermal fluid transfer systems using NN based models and rule based techniques," *Engineering Applications of Artificial Intelligence*, vol. 27, pp. 129–136, 2014.

[51] J. Andújar, F. Segura, and M. Vasallo, "A suitable model plant for control of the set fuel cell–DC/DC converter," *Journal of Renewable Energy*, vol. 33, no. 4, pp. 813–826, 2008.

[52] Ballard, "FCgen1020-ACS fuel cell from Ballard Power Systems," http://www.ballard.com/docs/default-source/backup-power-documents/fcgen-1020acs.pdf, 2018.

[53] V. Mehta and J. S. Cooper, "Review and analysis of PEM fuel cell design and manufacturing," *Journal of Power Sources*, vol. 114, no. 1, pp. 32–53, 2003.

[54] T. R. Ralph, G. A. Hards, J. E. Keating et al., "Low cost electrodes for proton exchange membrane fuel cells: Performance in single cells and ballard stacks," *Journal of The Electrochemical Society*, vol. 144, no. 11, pp. 3845–3857, 1997.

[55] Ballard, "FCgenTM-1020ACS/FCvelocityTM-1020ACS Fuel Cell Stack. Ballard Product Manual and Integration Guide," Document Number MAN5100192-0GS, 2009.

[56] F. Segura and J. Andújar, "Step by step development of a real fuel cell system. Design, implementation, control and monitoring," *International Journal of Hydrogen Energy*, vol. 40, no. 15, pp. 5496–5508, 2015.

[57] F. Segura and J. Andújar, "Modular pem fuel cell scada & simulator system," *Resources*, vol. 4, no. 3, pp. 692–712, 2015.

[58] F. Segura, V. Bartolucci, and J. Andújar, "Hardware/software data acquisition system for real time cell temperature monitoring in air-cooled polymer electrolyte fuel cells," *Sensors*, vol. 17, no. 7, article no. 1600, 2017.

[59] X. Li, Z. Deng, D. Wei et al., "Parameter optimization of thermal-model-oriented control law for PEM fuel cell stack via novel genetic algorithm," *Energy Conversion and Management*, vol. 52, no. 11, pp. 3290–3300, 2011.

[60] J. MacQueen, "Some methods for classification and analysis of multivariate observations," in *Proceedings of the Berkeley Symposium on Mathematical Statistics and Probability, Volume 1: Statistics*, vol. 1, pp. 281–297, 1967.

[61] J. Moody and C. J. Darken, "Fast learning in networks of locally-tuned processing units," *Neural Computation*, vol. 1, no. 2, pp. 281–294, 1989.

[62] J. Orallo, M. Quintana, and C. Ramírez, *Introducción a la Minería de Datos*, Editorial Alhambra, S.A., 2004.

[63] P. Viñuela and I. León, *Redes De Neuronas Artificiales: Un Enfoque Práctico*, Pearson Educación - Prentice Hall, 2004.

[64] M. Galipienso, M. Quevedo, O. Pardo et al., *Inteligencia Artificial. Modelos, Técnicas Y Áreas De Aplicación*, Editorial Paraninfo, 2003.

[65] J. González and V. Hernando, *Redes Neuronales Artificiales: Fundamentos, Modelos Y Aplicaciones*, RA-MA, 1995.

[66] A. M. C. Harston and R. Pap, *Handbook of Neural Computing Applications*, Elsevier, 2014.

[67] B. Del Brío and A. Molina, *Redes Neuronales Y Sistemas Borrosos*, RA-MA, 2006.

[68] R. López and J. Fernández, *Las Redes Neuronales Artificiales*, Netbiblo, 2008.